A first-principles divide-and-conquer approach for electronic structure of large systems and its application to graphene nanoribbons

2009 J. Phys.: Condens. Matter 21 235501

(http://iopscience.iop.org/0953-8984/21/23/235501)

IOP PUBLISHING JOURNAL OF PHYSICS: CONDENSED MATTER

J. Phys.: Condens. Matter **21** (2009) 235501 (5pp) doi:10.1088/0953-8984/21/23/235501

A first-principles divide-and-conquer approach for electronic structure of large systems and its application to graphene nanoribbons

Y X Yao, C Z Wang, G P Zhang, M Ji and K M Ho

Ames Laboratory-US DOE and Department of Physics and Astronomy, Iowa State University, Ames, IA 50011, USA

E-mail: wangcz@ameslab.gov

Received 25 February 2009, in final form 23 April 2009
Published 15 May 2009
Online at stacks.iop.org/JPhysCM/21/235501

Abstract

We demonstrate an efficient and accurate first-principles method to calculate the electronic structure of a large system using a divide-and-conquer strategy based on localized quasi-atomic minimal basis set orbitals recently developed. Tight-binding Hamiltonian and overlap matrices of a large system can be constructed by extracting the matrix elements for a given pair of atoms from first-principles calculations of smaller systems that represent the local bonding environment of the particular atom pair. The approach is successfully applied to the studies of electronic structure in graphene nanoribbons. This provides a promising way to do the electronic simulation for large systems directly from first principles.

(Some figures in this article are in colour only in the electronic version)

1. Introduction

First-principles methods based on density functional theory (DFT) [1] and plane-wave basis [2, 3] have been well developed over the past four decades and very successful in calculating the electronic structure and total energy of many systems. Nevertheless, due to the complexity of the algorithms and the fact that a large number of basis functions is required in the calculation, many complex structures and materials that require a computational unit cell containing thousands of atoms are still beyond the reach of first-principles plane-wave-based DFT methods.

On the other hand, considerable work has been done in trying to use localized orbitals as basis [4–10] in order to reduce the dimension of the Hamiltonian matrix, so that a large number of atoms can be handled in the calculation. It has also been shown that O(N) scaling in the first-principles calculations (i.e. the computational workload scales linearly with the number of atoms in the calculation) can be achieved by using a set of well-localized orbitals as basis [4–8, 10]. However, the efficiency and accuracy of the calculations in this approach strongly depend on the choice of basis orbitals. In many cases, accurate calculations would require a basis set consisting of a large number of localized orbitals which slow down the calculations considerably [10]. Thus it is highly desirable to have a set of localized minimal basis orbitals that can faithfully reproduce the converged occupied electronic structure.

Recently two independent approaches, i.e. the maximally localized Wanier functions approach by Marzari and Vanderbilt [11] and the quasi-atomic minimal basis set orbitals (QUAMBOs) approach by Lu *et al* [12–14], demonstrated that highly localized minimal basis set orbitals can be constructed through unitary transformations of the wavefunctions obtained from fully self-consistent first-principles calculations with a large basis set. These minimal basis set orbitals are atomic-like but deform according to the bonding environment, and can span exactly the same preserved electronic subspace as the full-basis first-principles calculations. These minimal basis sets would serve as a promising platform for developing an efficient yet accurate method for large scale electronic calculations.

In this paper, we show that accurate tight-binding Hamiltonians and overlap matrix elements can be calculated by first-principles methods through the QUAMBO representation

of electronic structure at different local bonding environments. By sampling various local bonding environments of a large complex system from a series of first-principles calculations of smaller systems, the 'exact' environment-dependent tight-binding matrix of the large system can be assembled directly from a first-principles approach without resorting to the usual fitting procedure to generate tight-binding parameters.

2. Method

The method to project the QUAMBOs from the full-basis first-principles wavefunctions has been described in detail in our previous publications [12–14]. Starting with the wavefunction obtained from the full-basis first-principles calculations, the key steps in the QUAMBOs construction are (1) select all the occupied states or any set of states of interest to be preserved; (2) construct a small subset of virtual orbitals that are maximally coherent with the occupied states from the entire unoccupied subspace. This small subset of unoccupied orbitals represents the anti-bonding states which are not necessarily the lowest energy unoccupied states but rather linear combinations of the states in the entire virtual space that capture most of the anti-bonding orbital character. The number of selected virtual orbitals is equal to the difference between the number of minimal basis orbitals and the number of preserved occupied orbitals in the system; (3) combine the preserved occupied orbitals with the selected small subset of virtual orbitals to form the QUAMBO subspace. These localized quasi-atomic orbitals provide an accurate local minimal basis set from which tight-binding Hamiltonians and overlap matrices can be evaluated.

In our scheme for large scale electronic calculation, an overlap or tight-binding Hamiltonian matrix of a large system is built by filling in a set of $n \times m$ 'exact' sub-matrices of all pairs of atoms in the system, where n and m are the numbers of minimal basis orbitals for the two atoms in the pair, respectively. These $n \times m$ 'exact' sub-matrices are calculated from first principles following the QUAMBO procedure described above. Note that the QUAMBOs, and hence the $n \times m$ sub-matrices of tight-binding, are dependent on the environment around the pair of atoms, and in principle the $n \times m$ 'exact' sub-matrices have to be calculated for every pair of atoms in the system. This can be done by first performing first-principles calculations for a relatively small system which keeps the dominant local environment of the pair of atoms in the large system; then the $n \times m$ tight-binding matrix for this pair of atoms can be constructed following the QUAMBO scheme. This approach will break the first-principles calculations of a large system into many much smaller subsystem calculations. In many cases of interest (e.g. defects in crystals), the bonding environment of many different atom pairs in the large system are essentially the same. Therefore, in practice first-principles calculations are needed only for a limited number of smaller systems and an accurate tight-binding overlap and Hamiltonian matrices for the large system can be constructed. The scheme was illustrated with a study of the electronic structure of graphene nanoribbons.

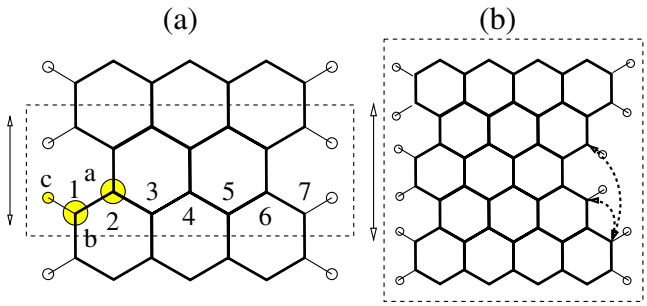

Figure 1. (a) $N_a = 7$ A-GNR was chosen to be the training sample for perfect A-GNR. The dotted rectangle indicates the primitive unit cell. The left arrow gives the periodic direction. Atoms a, b and c are treated to be three different atoms according to their local environment. (b) Additional training sample for studies on A-GNRs with edge defects.

3. Results

We first applied our scheme to calculate the electronic structure of perfect armchair-graphene nanoribbons (A-GNRs) of different widths, where three different types of atoms in the nanoribbons have been identified as shown in figure 1(a): atom a represents a carbon atom inside the ribbon, atom b represents a carbon atom at the edge and atom c is a hydrogen atom for passivation. The number of minimal basis orbitals for a carbon atom is 4 (one s and three p) and that for a hydrogen atom is 1. Only one training cell of $N_a = 7$ A-GNR as shown in figure 1(a) and a single first-principles calculation is needed to extract all the necessary 'exact' 4×4 or 4×1 tight-binding matrices for each pair of a–a, a–b, b–b and b–c atoms from these three types of non-equivalent atoms, respectively. We notice that the same type of atom pair by our definition (i.e. a–a, a–b, b–b and b–c) can appear more than once at different locations in the same training cell (or in different training cells) and, strictly speaking, their bonding environments are not exactly the same. But we found the tight-binding hopping elements of the same type of pairs are different only on the order of several meV, while the overlapping elements are almost the same. Therefore, we assign the matrix elements to each type of atom pair in the system by taking an algebraic average over the same type of pairs in the training cells. All the occupied states and some π^* antibonding states up to 4 eV above the Fermi level are preserved in the QUAMBO construction. Figure 2 shows the band structures for A-GNRs with width $N_a = 7$ and 13 (solid lines) from the QUAMBO tight-binding scheme using small 4×4 and 4×1 tight-binding matrices generated from the $N_a = 7$ training cell as described above. The results from full first-principles calculations (circles) were also shown for comparison. One can see that the QUAMBO-TB band structures agree very well with the full first-principles results in the targeted energy window. One may observe some additional DFT bands between 3 and 4 eV above the Fermi level. These bands are dominated by higher angular momentum characters, so they are not covered by the tight-binding results with minimal basis (s, p). (However, one can always include more orbitals in QUAMBO construction to capture these relatively higher-energy bands if

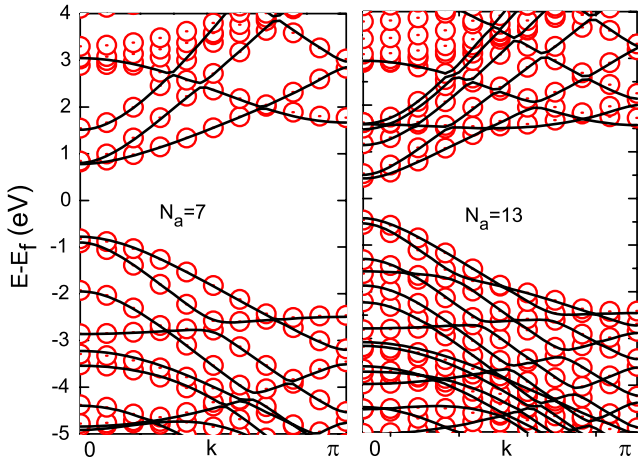

Figure 2. Band structures based on the QUAMBO-TB scheme (solid line) compared with DFT results (circle) for A-GNR with $N_a = 7$ and 13.

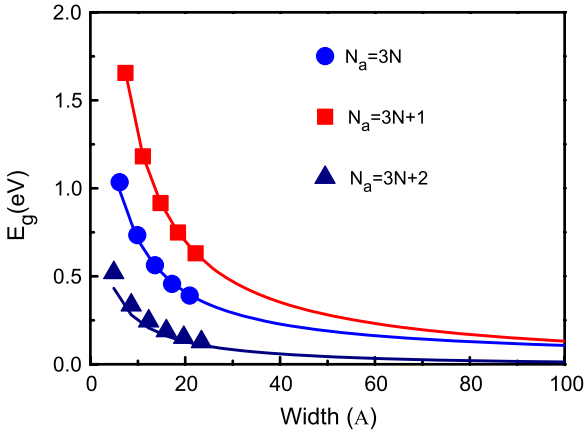

Figure 3. TB bandgap (solid lines) of A-GNR with different size compared with DFT results (symbols).

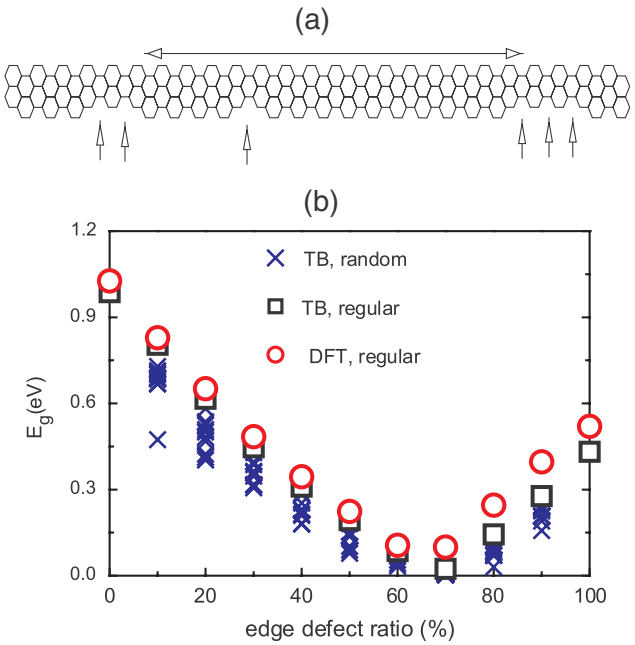

Figure 4. (a) Schematic view of a part of a supercell of $N_a = 6$ A-GNR containing more than one thousand atoms with edge defects randomly distributed on one side. Small arrows indicate the edge defects. (b) Bandgap behavior of the defected $N_a = 6$ A-GNR with increasing edge defect ratio. The perfect $N_a = 6(5)$ A-GNR corresponds to a defect ratio of 0% (100%). Crosses are the results from supercells (containing 100 primitive unit cells of perfect A-GNR) with random edge defects. Squares (circles) are TB (DFT) results from smaller supercells (containing 10 primitive unit cells of perfect A-GNR) with regular edge defects by removing pairs of carbon atoms successively on one side.

desired.) The electronic bandgap variation of a perfect A-GNR as a function of the width of the nanoribbon has also been studied. Figure 3 shows the oscillation of the bandgap with a period of $N_a = 3$ obtained from our QUAMBO-TB scheme, which agrees very well with the results from first-principles calculations [16]. The efficiency of the QUAMBO-TB scheme enables us to calculate the electronic structure of much wider graphene nanoribbons, as one can also see from figure 3, where the bandgap of nanoribbons up to 100 Å in width has been calculated with our QUAMBO-TB method.

The QUAMBO-TB scheme also enables us to study the electronic structure of graphene nanoribbons with random defects. For the purpose of illustration, we have studied the electronic structures of $N_a = 6$ A-GNR with random edge defects on one edge of the ribbon at different concentrations. We first constructed a supercell of $N_a = 6$ A-GNR by repeating the primitive unit cell 100 times (containing 1200 carbon atoms). The edge defects were generated by randomly removing pairs of carbon atoms on one side as shown in figure 4(a). The new structures were passivated with hydrogen atoms. For this defect system, some additional QUAMBO-TB matrix elements around the edge defects are needed. We used another training cell as shown in figure 1(b) to obtain these additional matrix elements, where the curved arrows indicate the new matrix elements between these sites to be added to the existing QUAMBO-TB matrix elements' database from the $N_a = 7$ training cell as discussed above. Based upon this set of QUAMBO-TB matrix elements from first-principles calculations performed on two small unit cells as shown in figure 1, actual tight-binding overlap and Hamiltonian matrices for the defected graphene nanoribbons at various defect concentrations can be constructed and the electronic structure of A-GNRs with random edge defects can be studied. The results of the bandgap as a function of defect ratio in the $N_a = 6$ A-GNR are shown in figure 4(b). The random distribution of the edge defects gives some variation of the bandgap at each defect concentration: however, there exists a general trend of the bandgap with increasing defect concentration. The bandgap reaches its minimum (which is quite small) at a defect ratio of 70%. This implies that edge defects have a significant effect on the electronic structures of A-GNRs, which is consistent with observations from experiments [17]. In order to verify the accuracy of our QUAMBO-TB approach for studying the A-GNR with edge defects, we compared the QUAMBO-TB and DFT results of bandgaps as a function of the edge defect ratio for an $N_a = 6$ A-GNR with the edge defects regularly arranged in a much smaller supercell (so

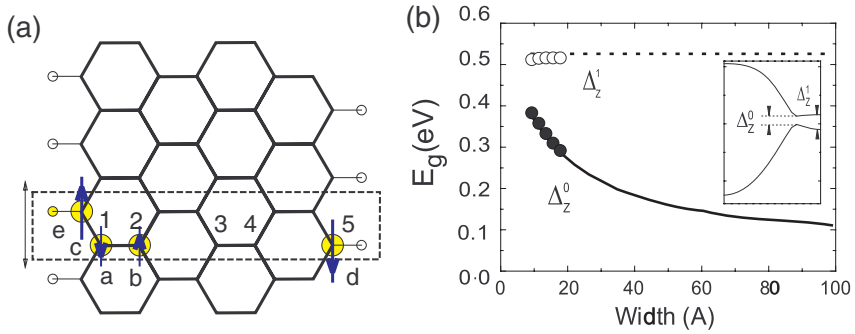

Figure 5. (a) The training sample for Z-GNRs. (b) TB bandgap (solid lines) of Z-GNR with different sizes compared to DFT results (symbols).

that DFT calculations can be easily performed). The lattice vector along the ribbon direction is only 10 times that of the primitive unit cell of an $N_a = 6$ A-GNR. The edge defects were constructed by removing pairs of carbon atoms successively on one side of the ribbon so that all the edge defects stay together in the supercell. The results are also shown in figure 4(b) where the open squares represent the results from our QUAMBO-TB and the open circles represent the results from full-basis DFT calculations. The results from the TB and the DFT agree with each other very well, indicating that the QUAMBO-TB approach we used in this study should be accurate for studying graphene nanoribbons with defects. It is also interesting to note from figure 4(b) that randomly distributed edge defects tend to have smaller bandgaps as compared to the case of regularly distributed defects at the same defect ratio.

Furthermore, the QUAMBO-TB scheme may also be applied to studies with spin polarization, where two sets of TB parameters (for spin-up and spin-down) are needed [14]. For a demonstration, we applied it to zigzag-graphene nanoribbons (Z-GNRs) which have a ground state with a spin configuration of FM-A, i.e. the coupling of spins is of ferromagnetic type at each edge and of antiferromagnetic type between the two edges [15, 16, 18]. Five different types of atoms in the nanoribbons have been identified as illustrated in figure 5(a), where atom a (b) represents a carbon atom inside the ribbon with spin-down (up) majority, atom c (d) represents a carbon atom at the edges with spin-up (down) majority and atom e is a hydrogen atom for passivation. Only one training sample of $N_z = 5$ Z-GNR as shown in figure 5(a) and a single first-principles calculation with local spin density approximation are needed to extract all the spin-up and spin-down tight-binding matrices for these five types of non-equivalent atoms. Figure 5(b) shows the bandgap behavior of Z-GNRs with width up to 100 Å. Lines are QUAMBO-TB results, which are consistent with DFT calculations indicated by circles [16]. It is very straightforward and advantageous to use our method to study the electronic structures of doped graphene nanoribbons [18] or graphene with adatom adsorption [19, 20].

4. Discussion

The success of our QUAMBO-based tight-binding divide-and-conquer approach relies on several fundamental physical concepts: local environmental dominance of physical properties [21], good localization and environmental adaptedness of the minimal basis set orbitals (QUAMBOs). The first locality property in materials is the physical foundation upon which the order-N methods may be developed [21]. For example, in Yang's density-based divide-and-conquer approach, the physical system may be divided into a few subsystems [22]. Also the charge density of each subsystem can be calculated separately. In our approach, the locality property ensures that a small training cell which keeps the local environment of certain atom pairs in large systems may be constructed. However, the exact size of the training cell depends on the specific systems. The training cell is expected to be relatively large for metallic systems.

The good localization and environmental adaptedness of QUAMBOs make the derived tight-binding parameters short-ranged as well as exact. Namely, the converged electronic structure with respect to the basis set may be exactly downfolded into a short-ranged tight-binding representation, which is pioneered by Andersen in his muffin-tin orbitals approach [23]. Therefore only smaller numbers of atom pairs and training cells need to be considered. In the case of perfect A-GNRs, one training cell actually contains all the necessary tight-binding parameters.

Our scheme does not explicitly include the atomic relaxation. However, the lattice distortion effect is readily taken care of by the proper choice of training cells. The current scheme is mainly focused on the electronic structure calculation of large systems. The total energy and its derivatives cannot be obtained. Hence the total energy calculations and molecular dynamics may not be handled. However, the scheme may be further developed following the way of traditional tight-binding potential development.

5. Conclusion

We have demonstrated an efficient and accurate method for calculating the electronic structure of a large system using a divide-and-conquer strategy. First-principles calculations are needed only for small numbers of atoms around the pairs, yet an accurate QUAMBO-TB matrix can be constructed for the whole system. Such an approach has proved quite successful for studies of the electronic structure in graphene nanoribbons.

This 'QUAMBO-on-demand' approach opens a promising avenue to do electronic structure simulations and total energy calculations for large systems directly from first principles.

Acknowledgments

Ames Laboratory is operated for the US Department of Energy by Iowa State University under contract no. DE-AC02-07CH11358. This work was supported by the Director for Energy Research, Office of Basic Energy Sciences, including a grant of computer time at the National Energy Research Supercomputing Center (NERSC) in Berkeley.

References

[1] Hohenberg P and Kohn W 1964 *Phys. Rev.* **136** B864
Kohn W and Sham L J 1965 *Phys. Rev.* **140** A1135
[2] Ihm J, Zunger A and Cohen L 1979 *J. Phys. C: Solid State Phys.* **12** 4409
[3] Payne M C, Teter M P, Allan D C, Arias T A and Joannopoulos J D 1992 *Rev. Mod. Phys.* **64** 1045
[4] Galli G and Parrinello M 1992 *Phys. Rev. Lett.* **69** 3547
[5] Mauri F, Galli G and Car R 1993 *Phys. Rev.* B **47** 9973
[6] Ordejon P, Drabold D A, Grumbach M P and Martin R M 1993 *Phys. Rev.* B **48** 14646
[7] Kim J, Mauri F and Galli G 1995 *Phys. Rev.* B **52** 1640
[8] Hernandez E and Gillan M J 1995 *Phys. Rev.* B **51** 10157
[9] Koepernik K and Eschrig H 1999 *Phys. Rev.* B **59** 1743
[10] Soler J M, Artacho E, Gale J, Garcia A, Junquera J, Ordejon P and Sanchez-Portal D 2002 *J. Phys.: Condens. Matter* **14** 2745
[11] Marzari N and Vanderbilt D 1997 *Phys. Rev.* B **56** 12847
[12] Lu W C, Wang C Z, Schmidt M W, Bytautas L, Ho K M and Ruedenberg K 2004 *J. Chem. Phys.* **120** 2629
Lu W C, Wang C Z, Schmidt M W, Bytautas L, Ho K M and Ruedenberg K 2004 *J. Chem. Phys.* **120** 2638
[13] Lu W C, Wang C Z, Chan T L, Ruedenberg K and Ho K M 2004 *Phys. Rev.* B **70** 041101(R)
Lu W C, Wang C Z, Ruedenberg K and Ho K M 2004 *Phys. Rev.* B **72** 205123
Chan T L, Yao Y X, Wang C Z, Lu W C, Li J, Qian X F, Yip S and Ho K M 2007 *Phys. Rev.* B **76** 205119
[14] Qian X F, Li J, Qi L, Wang C Z, Chan T L, Yao Y X, Ho K M and Yip S 2008 *Phys. Rev.* B **78** 245112
[15] Nakada K, Fujita M, Dresselhaus G and Dresselhaus M S 1996 *Phys. Rev.* B **54** 17954
[16] Son Y W, Cohen M L and Louie S G 2006 *Phys. Rev. Lett.* **97** 216803
[17] Han M Y, Ozyilmaz B, Zhang Y and Kim P 2007 *Phys. Rev. Lett.* **98** 206805
[18] Martins T B, Miwa R H, da Silva A J R and Fazzio A 2007 *Phys. Rev. Lett.* **98** 196803
[19] Duplock E J, Scheffer M and Lindan P J D *Phys. Rev. Lett.* **92** 225502
[20] Mao Y, Yuan J and Zhong J 2008 *J. Phys.: Condens. Matter* **20** 115209
[21] Goedecker S 1999 *Rev. Mod. Phys.* **71** 1085
[22] Yang W 1991 *Phys. Rev. Lett.* **66** 1438
[23] Andersen O K and Jepsen O 1984 *Phys. Rev. Lett.* **53** 2571
Andersen O K and Saha-Dasgupta T 2000 *Phys. Rev.* B **62** R16219
Andersen O K, Saha-Dasgupta T, Tank R W, Arcangeli C, Jepsen O and Krier G 2000 *Lect. Notes Phys.* **535** 3